X-ray and Neutron Reflectivity Studies of Styrene–Maleic Acid Polymer Interactions with Galactolipid–Containing Monolayers

Article *in* Biophysical Journal · February 2020

DOI: 10.1016/j.bpj.2019.11.664

7 authors, including:

Minh D Phan
Oak Ridge National Laboratory
16 PUBLICATIONS **67** CITATIONS
SEE PROFILE

Olena Korotych
University of Tennessee
8 PUBLICATIONS **124** CITATIONS
SEE PROFILE

Nathan G. Brady
University of Tennessee
8 PUBLICATIONS **23** CITATIONS
SEE PROFILE

John F Ankner
Oak Ridge National Laboratory
175 PUBLICATIONS **2,654** CITATIONS
SEE PROFILE

European Polymer Journal 111 (2019) 178–184

Contents lists available at ScienceDirect

European Polymer Journal

journal homepage: www.elsevier.com/locate/europolj

Analysis of styrene maleic acid alternating copolymer supramolecular assemblies in solution by small angle X-ray scattering

Nathan G. Brady[a], Shuo Qian[b,c], Barry D. Bruce[a,d,*]

[a] Department of Biochemistry and Cellular & Molecular Biology, University of Tennessee, Knoxville, TN, USA
[b] Neutron Sciences Directorate, Oak Ridge National Laboratory, Oak Ridge, TN, USA
[c] Center for Structural Molecular Biology, Oak Ridge National Laboratory, Oak Ridge, TN, USA
[d] Department of Genome Sciences and Technology, University of Tennessee Knoxville, TN, USA

ARTICLE INFO

Keywords:
Styrene maleic acid (SMA)
Styrene maleic acid lipid particle (SMALP)
Small angle X-ray scattering (SAXS)
Supramolecular assembly
Amphiphilic polymer
Membrane protein solubilization

ABSTRACT

Over the past decade, Styrene Maleic Acid alternating copolymers (SMA) have gained interest as an alternative to detergent solubilization for the isolation of integral membrane proteins. The formation of SMA lipid particles (SMALPs) presents a novel opportunity to isolate the proximal membrane environment, encompassing and throughout membrane proteins *in vitro*. Neither the organization or structure of SMAs in an aqueous buffer nor the mechanism by which SMA transforms the membrane bilayer into a SMALP is known. This study investigates the shape and size of diverse SMA polymer complexes/aggregates in solution at various pH, ionic strength, SMA concentration and temperature, analyzed by small angle X-ray scattering. It is clear that SMAs of differing physicochemical properties (styrene to maleic acid ratio, length of copolymer fragments and functionalization) display highly variable sizes/shapes in solution over a range of environmental conditions. The SMA supramolecular aggregates exhibit similar prolate ellipsoidal geometry of varying size, dependent on the degree of hydrophobicity of the SMA copolymer. At elevated temperature, particles composed of SMAs enriched in styrene increase in both radius of gyration and maximum particle diameter. Interestingly, we observe a correlation between the SMALP dimensions and that of native membranes. Future work will investigate if there may be a complimentary relationship between SMA aggregate dimensions and bilayer thickness (and/or protein transmembrane domain thickness), similar to what has been observed for tandem facial amphiphiles.

1. Introduction

An estimated 20–30% of all genes across known genomes encode for membrane bound proteins [1]. These proteins perform many critical functions including the transmembrane trafficking of electrons, protons, ions and molecules, photonic energy conversion and signal transduction to name a few. Approximately one third of all known eukaryotic proteins are integrated into membranes, and are the target for approximately 40% of drugs on the market today [2]. Despite the ubiquitous nature of these proteins and their importance in medicine, there exists a severe shortage of structural information for membrane proteins as compared to soluble proteins. As of June 2018, less than 3.5% of the over 140,000 proteins that comprise the Protein Data Bank, exist on or within a membrane [3]. This disparity stems from the difficulties encountered in the isolation of membrane proteins from their native lipid environments. During the canonical method of membrane solubilization via surfactant-lipid exchange, detergents have been shown to replace membrane lipids peripheral and interior to membrane bound proteins [4]. Obstacles in the crystallization of membrane proteins, for example, may be due to partial denaturation of the protein during solubilization with detergent [5,6]. Detergents in their monomeric form bind to relatively small, contained hydrophobic regions in a saturable manner, however detergent micelles can cause proteins to unfold [7]. Detergents have also been shown to replace lipids that reside in specific lipid binding pockets, interior to membrane protein oligomeric complexes [4]. These lipids have been theorized to be critical to the topology, positioning of helices, assembly and oligomerization of these protein complexes. Further, native lipids have been posited to be involved in the stabilization of cofactors and may mediate electron and/or proton transfer, via alteration of the dielectric constant

Abbreviations: CV, Cray Valley; P(R), distance distribution; I(Q), intensity of scattered X-rays; D_{MAX}, maximum particle diameter; MSPs, membrane scaffolding proteins; M_N, number averaged molecular weight; PS, Polyscope; R_g, radius of gyration; Q, scattering angle; SAXS, small angle X-ray scattering; S(Q), structure factor; SMA, styrene maleic acid; SMALP, styrene maleic acid lipid particle; S:MA, styrene to maleic acid ratio; M_W, weight averaged molecular weight

* Corresponding author at: 125 Austin Peay Bldg, University of Tennessee, Knoxville, TN 37996, USA.
E-mail addresses: nbrady2@vols.utk.edu (N.G. Brady), qians@ornl.gov (S. Qian), bbruce@utk.edu (B.D. Bruce).

https://doi.org/10.1016/j.eurpolymj.2018.11.034
Received 22 June 2018; Received in revised form 15 November 2018; Accepted 19 November 2018
Available online 20 November 2018
0014-3057/

between metal containing cofactors such as heme pairs [4]. Supporting these theories, the delipidation of the Na^+, K^+ -ATPase and cytochrome b_6f complexes, has resulted in monomerization and loss of enzyme activity [4,8–12].

Surfactant-lipid exchange via detergent solubilization has remained the canonical method for membrane protein isolation for the last 70 years. This process results in the solvation of hydrophobic surfaces of membrane proteins with detergents to produce water soluble protein-detergent complexes [13]. Many detergents have been synthesized and utilized to this end, and membrane proteins have proven to be more or less sensitive to the denaturing effects of detergent solubilization. Alkyl ionic detergents such as sodium dodecyl sulfate, for example, are almost always denaturing [14]. With any type of detergent solubilization, the membrane undergoes various states of disintegration, driven by detergent concentration. Solubilization of some membrane proteins can occur at ratios as low as 1:10 detergent to membrane lipid, leaving the bilayer membrane mostly intact. At approximate ratios of 2:1, solubilization of the membrane occurs, resulting in mixed lipid-detergent and detergent-lipid-protein micelles. And at ratios around 10:1 detergent to lipid, complete delipidation occurs, resulting in protein-detergent micelles, though exact ratios are dependent on the molecular properties of the detergent and the supramolecular aggregate formation of lipid-detergent micelles [14].

As our knowledge concerning the complexity of natural membrane systems grows, the implications they pose to the overall functionality and folding of the proteins embedded within them becomes increasingly apparent [15]. For this reason, there has been a movement in the field to refer to these proteins as “proteo-lipid complexes” underlining the criticality of these systems to be studied as a whole. In an attempt to simulate this environment, the advent of lipid nanodiscs emerged in 2003. This approach involves the detergent solubilization of membrane proteins, and subsequent insertion into nanodiscs of membrane mimetics bound by membrane scaffolding proteins, referred to as MSPs [16]. This technique, while an exciting innovation in the field, failed to eliminate the detrimental effects of detergent solubilization on membrane proteins, as well as the MSPs themselves presenting issues downstream for *in vitro* protein analysis [15]. At present, a powerful new tool has been added to the membrane biochemistry toolbox; SMA alternating copolymers. The isolation of membrane proteins within SMALPs, offers a novel opportunity to study membrane proteins while retaining their native lipid environment around and throughout these complexes.

This burgeoning SMALP field has produced promising results with this new technique over the past decade, leading to the synthesis of various SMA copolymers. Similar to detergents, these SMAs are amphiphilic copolymers, consisting of moieties of hydrophobic styrene and hydrophilic maleic acid. The physicochemical properties of these polymers have been varied in styrene:maleic acid ratio (S:MA) and length of polymer fragments, reported as a weight averaged molecular weight (M_W) or number averaged molecular weight (M_N). For the purposes of this study, M_W will be used to refer to copolymer length. Depicted in Fig. 1 are four SMAs that have been chosen to be the focus of this work. These SMAs come from two different manufacturers, Cray Valley (CV) and Polyscope (PS) and have been shown to be among the most effective in the formation of SMALPs.

Membrane proteins encompassed within these SMALPs have been reported to have many favorable characteristics compared to their detergent micelle predecessors. Numerous investigations have demonstrated enhanced stability and more native like biophysical characteristics of target proteins *in vitro* [2,12,17–23]. Increased thermal stability of SMALPs has also been reported, approaching 100 °C before denaturation [2,20,24]. Smaller M_W SMAs in the range of 7–10 kDa and S:MA ratios of 2:1 or 3:1 have been proposed to be most efficient for membrane protein solubilization, forming more stable SMALPs [24,25]. However larger M_W SMAs in the range of 80–120 kDa have been suggested as optimum for the extraction of larger protein oligomers [18]. Initial observations suggest there may be a minimum concentration of SMA in solution marking the point at which intercalation occurs and SMALPs are spontaneously formed [18,25,26]. Further, it has been shown that SMA is more efficient in protein extraction in more fluid membranes, meaning shorter acyl chain lengths (thinner membranes), decreased lateral packing pressures and at elevated temperature [27,28]. Interestingly, it has been reported that the affinity of SMA for lipid is so high, that under most experimental conditions following the formation of SMALPs, there remains no free SMA in solution over a wide range of polymer:lipid ratios [28]. As with any technique, SMA also displays some inherent drawbacks. Mainly, the vast majority of these amphiphilic polymers tested are insoluble at neutral to acidic pH [18,25]. At elevated pH, SMAs display a sensitivity to divalent cations, attributed to the stabilization of the deprotonated maleic acid functionality, causing self-aggregation of the polymer [20,24,29]. Another commonly reported feature of these copolymers is the need for high ionic strength, in the range of 100–500 mM monovalent ions [15,17,27,29].

In light of these new capabilities offered to the membrane community by the production of native nanodiscs, questions persist regarding the underlying mechanism behind the formation of SMALPs. Reported here is the characterization of a selected set of SMA copolymers by small angle X-ray scattering (SAXS), observed over varied sample conditions. In contrast to X-ray crystallography, SAXS is a technique that lacks atomic resolution. However, SAXS produces highly precise dimensional information regarding size and shape under biologically relevant solution conditions. In solution scattering experiments, it is the requirement for rotational averaging of the molecules that leads to limitations regarding internal atomistic structure determination, rather than the resolution of the technique [30]. Determining the behavior, transition points and overall dimensions of these SMA supramolecular aggregates, is central to building a conceptual model to explain more complex systems.

2. Materials and methods

2.1. Styrene maleic acid copolymers

SMA copolymers were obtained from Cray Valley (a Total company), Paris, France and Polyscope, Geleen, The Netherlands. The SMAs were in solution upon arrival, and wt% of the polymers (listed on Certificates of Analyses from the manufacturers) were confirmed gravimetrically in the laboratory following lyophilization. All SMAs in this study were then diluted into sample buffer to a final concentration of 1.7% (w/v), unless otherwise specified (as in Fig. 2B). Sample buffer consisted of 50 mM Tris-Cl at various pH and KCl concentration, specific for each experiment.

2.2. Small angle X-ray scattering

The SAXS experiments were performed on a Rigaku BioSAXS-2000 system with a rotating anode, producing Cu Kα X-ray radiation at 1.54 Å.

SAXS data were averaged and reduced using Rigaku SAXSlab data collection and processing software, and was loaded directly into PRIMUS for initial inspection and interfacing with size determination software [31]. R_g and D_{MAX} were calculated using the inverse Fourier transform method executed in GNOM [32].

3. Results

To obtain reliable results regarding radius of gyration (R_g) and maximum particle diameter (D_{MAX}) from small angle scattering data, particles must be monodisperse. Following data averaging and buffer subtraction, scattering curves from solutions containing the four SMA copolymers depicted in Fig. 1, were generated and plotted as intensity

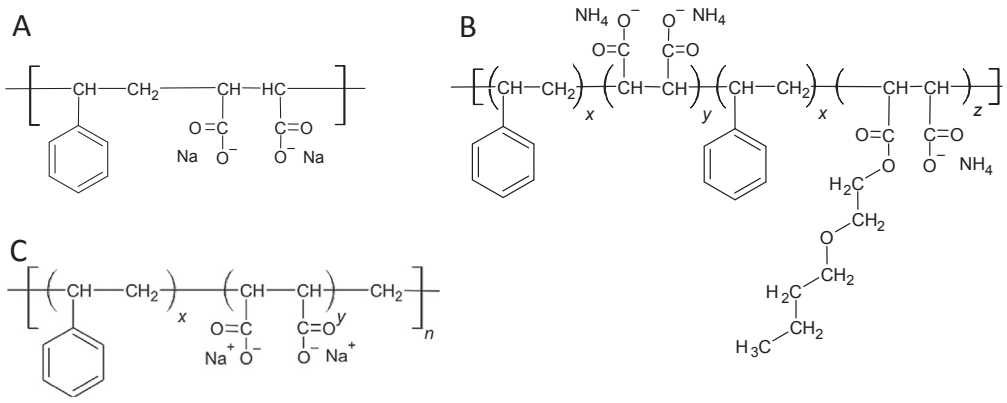

Fig. 1. Linear structure representations of four SMA copolymers used in this work, manufactured by Cray Valley (CV) and Polyscope (PS). A) CV-1000, S:MA = 1:1, M_W = 5.00 kDa, B) CV-1440, S:MA = 1.5:1, M_W = 7.00 kDa, C) PS-25010, S:MA = 3:1, M_W = 9.20 kDa and PS-30010, S:MA = 2:1, M_W = 6.50 kDa.

of the scattered X-rays; (I(Q)) against the scattering angle (Q) in a double logarithmic scale (Fig. 2). A decrease in intensity at lower scattering angle, presenting a maximum at larger Q, marks the presence of a structure factor (S(Q)) inherent in the system, suggesting interparticle correlation, also referred to as interparticle interference [33]. This S(Q) is caused by columbic repulsion between particles and can be seen to increase with increasing pH as the maleic acid groups become deprotonated (Fig. 2a). At pH = 9.53, this interparticle interference is alleviated by decreasing the concentration of SMA in solution, accompanied by an overall decrease in scattering signal (Fig. 2b). High concentrations of particles are known to produce interferent scattering signals. This occurs as the space between individual particles comes within range of the intraparticle distances [33].The interparticle interference can be eliminated by shielding the repulsive forces between carboxylate groups via the addition of monovalent ions (Fig. 2c). This addition of monovalent ions decreases the stability of the supramolecular aggregates overall, as interparticle repulsive forces are critical to the stability of colloids in solution. It is therefore imperative for SAXS experiments that interparticle repulsive forces be minimized, without causing sample aggregation. The severity of both of these effects can be observed upon an initial assessment of the scattering profile and optimal sample conditions can be determined. The presence of interparticle interference was seen across all SMA samples tested, exhibiting the same response as the representative samples depicted in Fig. 2.

Guinier analysis (Eq. (1)) was performed to obtain R_g of the SMA copolymers. The Guinier region exists at low Q values and is therefore most sensitive to the largest distances in the particle.

$$Ln(I(Q)) = Ln(I_0) - (R_g^2/3)Q^2 \quad (1)$$

In this analysis, R_g can be directly calculated from the slope of the linear regression obtained from Ln(I(Q)) versus Q^2 and the expression $m = R_g^2/3$. This relationship only holds true for regions where $QR_g < 1.3$ [30,34,35]. The presence of interparticle interference drives this approximation to report artificially low R_g values. Therefore, this approximation is only viable for curves that present maximum intensity at low Q, i.e. samples that do not exhibit a structure factor. Fig. 3 shows a representative Guinier plot from PS-30010, where the structure factor is fully mitigated by supplying sufficient ionic strength at 125 mM KCl.

From the initial scattering curves and Guinier analysis, significant interparticle interference was confirmed to be sufficiently alleviated at high ionic strength (Fig. 2C). Therefore, the following experiments were performed at 125 mM KCl to determine size dimensions of the SMA supramolecular aggregates. Indirect Fourier transformation of the entire scattering profile was performed to obtain the distance distribution (P(R)) at variable pH (Fig. 4) [30,32,36]. This P(R) function results in a histogram representation of all possible atom pair distances within the particle, and can provide further indications regarding interparticle interference or aggregation [33]. The D_{MAX} is depicted as the point at which this curve terminates at the x-axis. The arrival at Y = 0 should occur in a smooth and concave fashion, as an abrupt approach will lead to an underestimation of D_{MAX}, suggestive of interparticle interference [30]. Conversely, a P(R) distribution that extends asymptotically along the X-axis, leads to an overestimation of D_{MAX} and alludes to the presence of sample aggregation, or unfolded particles [30,37]. Further, the overall shape of the curve obtained by the P(R) distribution is indicative of the geometry of the supramolecular structures [38]. The SMAs tested in this study exhibit P(R) curves that are slightly asymmetrical with tailing at high R, which is representative of prolate ellipsoidal (egg shaped) particles (Fig. 4) [39]. The shoulders on the P(R) curve seen at low R in Fig. 4A and D depict the presence of smaller assemblies. Interestingly, this population of smaller particles occurs at different ends of the pH range tested for different SMA copolymers. This population of smaller particles is present at pH = 8.56 for CV-1000 (Fig. 4A) and at pH = 10.0 for PS-30010 (Fig. 4D).

The four SMA copolymers were then analyzed at 30, 40, 50 and 60 °C to probe for transitions in supramolecular aggregate structure. Both size parameters, R_g and D_{MAX} are shown graphically in Fig. 5. Across all conditions, CV-1440 forms larger particles than the other three polymers tested, which show similar dimensions over all conditions.

At sample conditions found to be optimum for SAXS analysis of these four copolymers (pH = 9.53 and 125 mM KCl), an additional set of 5 SMA formulations were successfully analyzed. The values for R_g and D_{MAX} are shown for these SMA copolymers in Table 1. These samples show a considerable size range, with D_{MAX} values spanning 37–89 Å under the selected testing conditions. Interestingly, both CV-2000 and CV-2625 formed particles within the same size range as CV-1440 (Fig. 5, Table 1).

The asymmetric shape of the distance distribution curves in Fig. 4, coupled with the tailing seen at high R, suggest a similar overall geometry of the SMA supramolecular aggregates; a prolate ellipsoid (also referred to as prolate spheroid). At 25 °C (Fig. 4), the D_{MAX} remains relatively constant and reproduceable, with the exception of CV-1440 at pH 8.56 (Fig. 4). This increase in Rg and D_{MAX} for CV-1440 at pH 8.56, may be caused by the butoxyethanol chain coming unburied from the core as the surface of the particle becomes less electronegative. Elevated temperature imparts significant changes to particle sizes. At 30 °C, smaller particles across all SMAs emerge, depicted as a shoulder at low R on the P(R) distribution curve. This population of smaller particles persists across all higher temperatures tested (Fig. 6). It has been suggested in the field that elevated temperature may be required for membrane protein isolation, owing to the fluidity of the membrane allowing for the intercalation of SMA copolymers [28]. However, the presence of these smaller supramolecular aggregates at elevated temperature may be required for SMA insertion into natural membranes, facilitating membrane protein isolation. This would explain why some

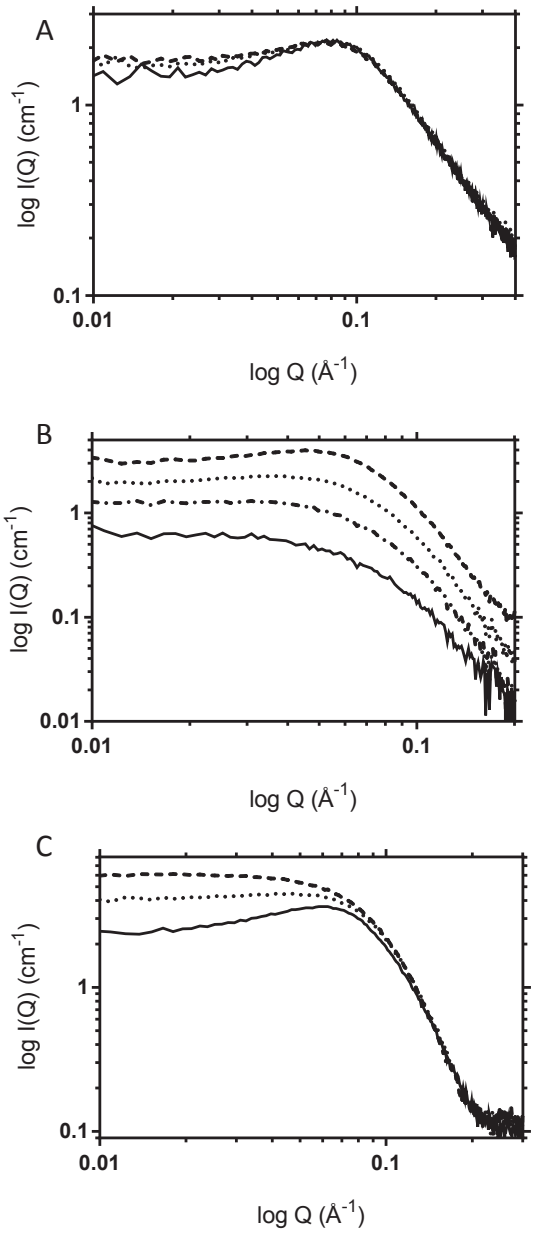

Fig. 2. Presence of structure factor in scattering signal. (A) 1.7% (w/v) CV-1000 measured at pH = 8.56 (dashed line), 9.53 (dotted line) and 10.0 (solid line). (B) CV-1440, pH = 9.53, 1.7% (w/v) (dashed line), 0.85% (w/v) (dotted line), 0.43% (w/v) (dashed/dotted line) and 0.17% (w/v) (solid line). (C) 1.70% (w/v) PS-25010, pH = 9.53, 125 mM KCl (dashed line), 50 mM KCl (dotted line) and no KCl (solid line).

SMAs are more effective at ambient temperature than others.

4. Conclusions and discussion

This study displays the utility of SAXS for the size determination of SMA copolymer supramolecular aggregates, given that interparticle repulsive forces can be sufficiently eliminated. This information can be used in conjunction with electrophoretic mobility data to obtain zeta potential of the SMA copolymer aggregates, in an attempt to better understand the way in which these assemblies will interact with membranes to facilitate protein extraction. It should be understood that the structure of these supramolecular aggregates is expected to change when mixed with native lipids. However, the extent to which SMA copolymers interact with free lipids or membrane systems, may be

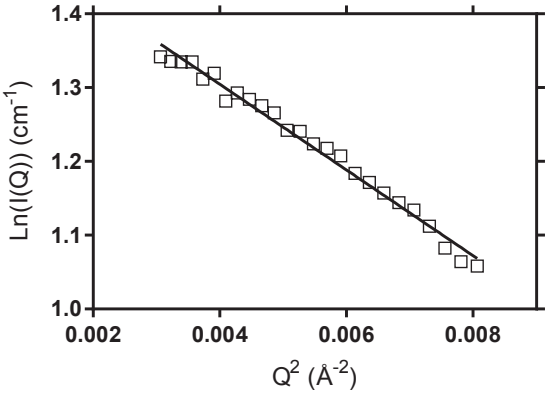

Fig. 3. Guinier plot of PS-30010 at pH = 9.53 and 125 mM KCl. The scattering curve at this ionic strength shows complete loss of structure factor, yielding a linear Guinier region and error within acceptable range, $QR_g < 1.3$.

dependent to some degree on the nature of the supramolecular aggregate assemblies.

The requirement for high ionic strength to facilitate membrane protein solubilization via SMA copolymers has been previously reported in the field [15,17,27,29]. The results presented here suggest significant interparticle repulsion forces at low ionic strength. The shielding effect provided by adequate amounts of monovalent ions, allow for true monodispersity of supramolecular aggregates in solution. This interparticle interference, caused by coulombic repulsive forces, suggests these SMA supramolecular aggregates exist in a formation where the hydrophilic maleic acid groups protrude from the particle and interact with the solvent. This is a logical hypothesis, that aligns with previous knowledge concerning micellular formation and coil to globular transition of polymers free in solution and is therefore not surprising. However, these experiments present the first evidence in support of this reasoning, confirming the occurrence of interparticle interference between SMA copolymer supramolecular aggregates over varying sample conditions. It is reasonable to infer that this state may be critical to allow for SMA interaction with membrane systems. Additionally, this information lends optimism that amphiphilic copolymers may behave similarly to detergents in solution with regard to critical transition concentrations, temperatures, ionic strength and counter ion preference, however further investigation is required to ascertain these criteria. Indeed, these properties of detergents in solution have been shown over the last 7 decades to be pertinent to the action of membrane protein solubilization, and the empirical results shown here suggest that this wealth of knowledge may be applicable to describing this new system of SMA copolymers. Further, with this roadmap of detergent properties as a guide, the prevalence of SAXS systems today allow this field a means for the rapid characterization of SMA copolymers over these ranges of environmental conditions, in a high throughput manner.

It has recently been reported that the topology of SMA copolymers, specifically the presence of a polystyrene enriched domain due to the RAFT synthesis technique, is advantageous to membrane protein solubilization [17]. Of the four SMA formulations chosen to be the focus of this work (Fig. 1), we see a similar topological effect regarding the formation of SMA supramolecular aggregates. CV-1440 has one significant difference in structure compared to the other copolymers analyzed; the presence of a butoxyethanol ester group. Across all conditions tested in this work, CV-1440 showed consistently larger R_g and D_{MAX} for the aggregates, as well as a smaller window of stability with regard to pH and temperature. This makes sense, as this SMA contains more hydrophobic groups to be buried in the core of the supramolecular aggregate, resulting in larger, less stable particles [40]. Where CV-1000, PS-25010 and PS-30010 yield comparable R_g and D_{MAX} over the pH ranges tested, CV-1440 exhibits larger sizes at low pH, presumably due to the butoxyethanol functional group becoming less buried from

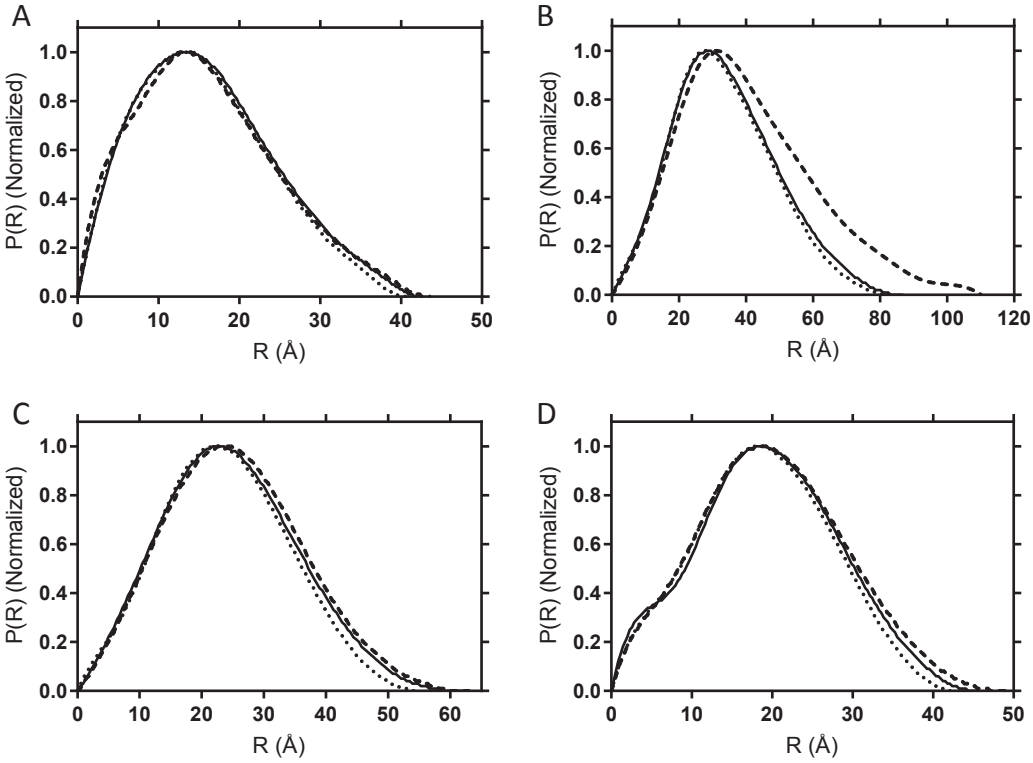

Fig. 4. Distance distribution analysis across entirety of the scattering profile at varying pH. SMA copolymers (A) CV-1000, (B) CV-1440, (C) PS-25010 and (D) PS-30010 were analyzed at pH = 8.56 (dashed line), pH = 9.53 (dotted line) and pH = 10.0 (solid line). All samples contained 125 mM KCl and were measured at 25 °C.

the core around pH = 8.5 (Figs. 4B and 5B).

With the exception of CV-1000, all SMAs show an increase in D_{MAX} at 60 °C, with PS-25010 and PS-30010 showing increases in D_{MAX} at 50 °C as well. CV-1000 shows no apparent change in geometry across all temperatures (Fig. 6A), owing to this formulation having an even 1:1 styrene:maleic acid ratio and the smallest fragments (M_W = 5.00 kDa, Fig. 1A). All other SMA copolymers are enriched in styrene compared to maleic acid and show a more pronounced change in supramolecular

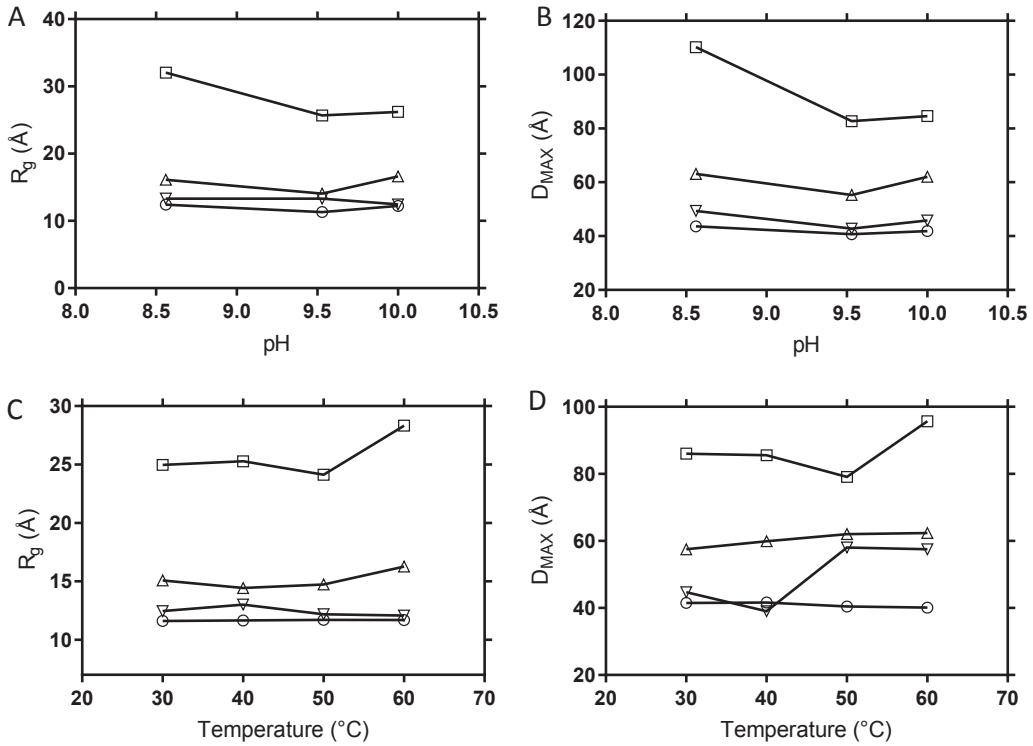

Fig. 5. R_g and D_{MAX} for SMA copolymers over varying pH (A and B) and temperature (C and D). For all plots the SMA copolymers are as follows: CV-1000 (circles), CV-1440 (squares), PS-25010 (triangles), PS-30010 (inverted triangles).

Table 1
R_g and D_{MAX} for additional SMA copolymers. All samples were tested with 125 mM KCl and pH = 9.53 at 25 °C.

SMA	Rg(Å)	D_{MAX} (Å)	S:MA	M_w	Counter Ion	Additional Functionalization
CV-2000	23.78	77.43	2:1	7.50	Ammonium	None
CV-2625	26.14	88.62	2:1	9.00	Ammonium	Partially esterified, 1-propanol
CV-10235	13.97	49.10	1.5:1	7.00	Ammonium	None
CV-17352	18.02	63.06	1.7:1	7.00	Ammonium	None
PS-40005	10.22	37.20	1.4:1	5.00	Sodium	None

structure with increasing temperature. These results are in line with previously published findings that report hydrophobic interactions to be most critical in stabilizing the globular or collapsed supramolecular state of SMA in solution, as compared to intramolecular hydrogen bonding [41,42]. Further, it has also been reported in the literature that this collapsed supramolecular structure is required for insertion into membranes to facilitate membrane protein extraction [43]. However, due to the random nature by which most SMA copolymers are synthesized, whether this collapsed conformation is driven by multiple hydrophobic domains or a single styrne enriched region remains to be elucidated [43]. Synthesis of these polymers in a more controlled manner, such as RAFT polymerization as previously discussed, may lend insight into this question of overall copolymer topology. SMA obtained from Polyscope show an increase in particle size occurring at lower temperatures than those obtained from Cray Valley (Fig. 6). This change in response to rising temperature may be caused by differences in copolymer structure with regard to regions of styrene enrichment, which could arise from variable synthesis methods. Another interesting observation is that in all cases except PS-30010, the R_g tracks relative to the D_{MAX} over variable pH and temperature (Fig. 5). Supramolecular aggregates of PS-30010 show a decrease in R_g correlating to an increase in D_{MAX} at $9.53 \leq pH \leq 10.0$ and temperatures between 40 °C and 60 °C. This effect is more subtle over variable pH, where an abrupt spike can be seen over varying temperature (Fig. 5). Taken together, these data suggest that the topology of the SMA copolymer changes the hydrophobic core, which in turn determines the size of the supramolecular aggregate, and the size of this structure over various sample conditions.

At present, there is no clear consensus in the field regarding which physicochemical properties (e.g. S:MA, M_W) of SMA copolymers are optimal for membrane protein extraction. The results presented here demonstrate that the dimensions of various SMA supramolecular aggregates vary greatly under diverse sample conditions. Therefore, the relative effectiveness of SMA formulations for this purpose may correlate with the size of these supramolecular aggregates free in solution, as it relates to the thickness of the membrane. This hypothesis requires further testing, however it is not without precedent in the literature. A recent study by Das et al. published in 2018, reports on the rational engineering of a new class of detergents for membrane protein extraction, termed tandem facial amphiphiles. This study concludes that the most effective tandem face maltoside detergents contained lipophilic groups approximately 31 Å in length, a size equal to the hydrophobic thickness of the target membrane in this study [44]. Discerning the underlying mechanism of SMALP formation will not only allow for the optimization of this process via copolymer design, but may also lead to specificity of protein targeting in complex natural membranes.

5. Data statement

The raw data required to reproduce these findings are available to download from this link. The processed data required to reproduce these findings are available to download from this link.

Acknowledgements

We thank Stefan Scheidelaar and Pieter Hanssen from Polyscope Polymers, Geleen, The Netherlands, for providing SMA copolymers and their support to our research and the SMALP community. We also thank Bill Dougherty from Cray Valley, Exton, Pennsylvania, USA for

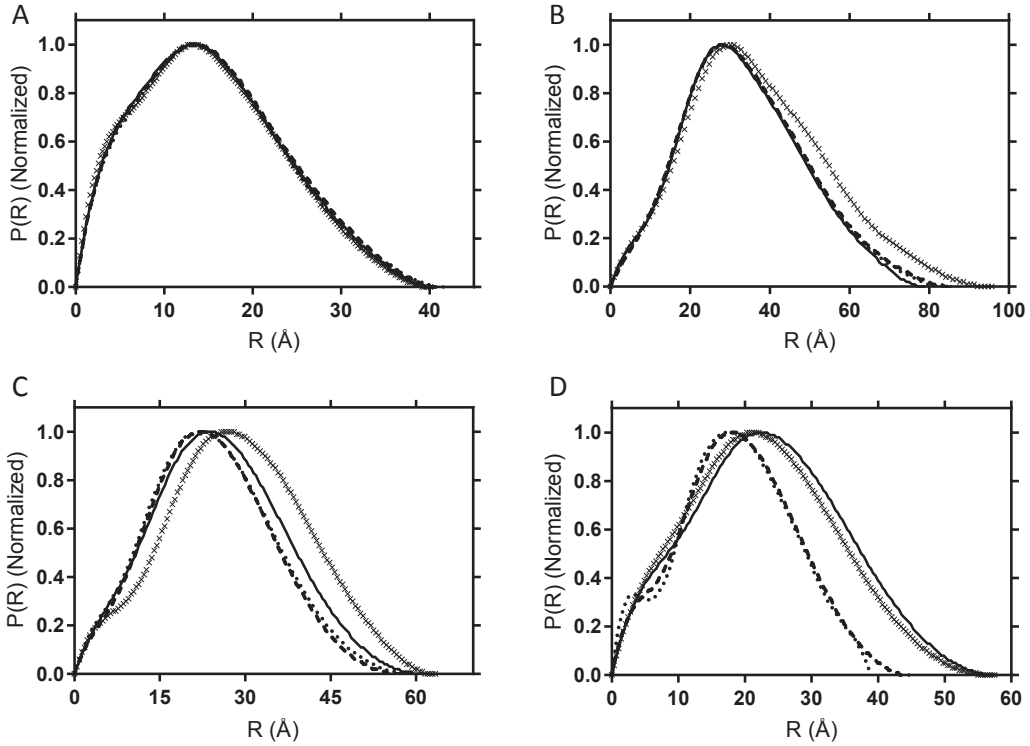

Fig. 6. Distance distribution analysis across entirety of the scattering profile at varying temperature. SMA copolymers A) CV-1000, B) CV-1440, C) PS-25010 and D) PS-30010 were analyzed at 30 °C (dashed line), 40 °C (dotted line), 50 °C (solid line) and 60 °C (X symbols). All samples contained 1.7% (w/v) SMA and 125 mM KCl.

providing SMA copolymer samples used in this work. The materials and technical expertise allowed us from these two companies allows this work to be possible. We would also like to thank Dr. Olena Korotych for her critical review of this manuscript, and aid in interpretation of these results. SAXS measurements were supported by DOE scientific user facilities at ORNL. Funding for CSMB is provided by the Office of Biological & Environmental Research in the *Department of Energy's Office of Science*. Support to B.D.B. and N.G.B. has been provided from the Gibson Family Foundation, the UTK/ORNL Science Alliance, the Tennessee Plant Research Center, JDRD Award to B.D.B., the Dr. Donald L. Akers Faculty Enrichment Fellowship to B.D.B. and National Science Foundation support to B.D.B. (DGE-0801470 and EPS-1004083). N.G.B. was also supported by the Penley Foundation Fellowship. Access to SAXS at ORNL was supported by a HIFR Beam Time Award 20149. These funding sources were not involved in data collection, analysis, interpretation or report writing.

Declaration of interest

None.

Appendix A. Supplementary material

Supplementary data to this article can be found online at https://doi.org/10.1016/j.eurpolymj.2018.11.034.

References

[1] A. Krogh, et al., Predicting transmembrane protein topology with a hidden Markov model: application to complete genomes, J. Mol. Biol. 305 (3) (2001) 567–580.
[2] T.J. Knowles, et al., Membrane proteins solubilized intact in lipid containing nanoparticles bounded by styrene maleic acid copolymer, J. Am. Chem. Soc. 131 (22) (2009) 7484–7485.
[3] H.M. Berman, et al., The protein data bank, Nucleic Acids Res. 28 (1) (2000) 235–242.
[4] S.S. Hasan, W.A. Cramer, Internal lipid architecture of the hetero-oligomeric cytochrome b6f complex, Structure 22 (7) (2014) 1008–1015.
[5] H. O'Neill, et al., Small-angle X-ray scattering study of photosystem I− detergent complexes: implications for membrane protein crystallization, J. Phys. Chem. B 111 (16) (2007) 4211–4219.
[6] J. Broecker, B.T. Eger, O.P. Ernst, Crystallogenesis of membrane proteins mediated by polymer-bounded lipid nanodiscs, Structure 25 (2) (2017) 384–392.
[7] D.E. Otzen, Protein unfolding in detergents: effect of micelle structure, ionic strength, pH, and temperature, Biophys. J. 83 (4) (2002) 2219–2230.
[8] M. le Maire, P. Champeil, J.V. MÖller, Interaction of membrane proteins and lipids with solubilizing detergents, Biochim. Biophys. Acta (BBA)-Biomembr. 1508 (1) (2000) 86–111.
[9] M. Esmann, J.C. Skou, C. Christiansen, Solubilization and molecular weight determination of the (Na+ + K+)-ATPase from rectal glands of Squalus acanthias, Biochim. Biophys. Acta (BBA)-Enzymol. 567 (2) (1979) 410–420.
[10] M. Esmann, The distribution of C12E8-solubilized oligomers of the (Na+ + K+-ATPase, Biochim. Biophys. Acta (BBA)-Protein Struct. Mol. Enzymol. 787 (1) (1984) 81–89.
[11] C. Breyton, et al., Dimer to Monomer Conversion of the Cytochromeb 6 f Complex CAUSES AND CONSEQUENCES, J. Biol. Chem. 272 (35) (1997) 21892–21900.
[12] M. Wheatley, et al., GPCR-styrene maleic acid lipid particles (GPCR-SMALPs): their nature and potential, Biochem. Soc. Trans. 44 (2) (2016) 619–623.
[13] A.J. Wolfe, et al., Quantification of membrane protein-detergent complex interactions, J. Phys. Chem. B 121 (44) (2017) 10228–10241.
[14] A. Helenius, et al., [63] Properties of detergents, Methods in Enzymology, Elsevier, 1979, pp. 734–749.
[15] S.C. Lee, et al., A method for detergent-free isolation of membrane proteins in their local lipid environment, Nat. Protoc. 11 (7) (2016) 1149.
[16] I. Denisov, et al., Directed self-assembly of monodisperse phospholipid bilayer Nanodiscs with controlled size, J. Am. Chem. Soc. 126 (11) (2004) 3477–3487.
[17] S.C.L. Hall, et al., Influence of Poly(styrene- co-maleic acid) Copolymer Structure on the Properties and Self-Assembly of SMALP Nanodiscs, Biomacromolecules 19 (3) (2018) 761–772.
[18] M. Esmaili, M. Overduin, Membrane biology visualized in nanometer-sized discs formed by styrene maleic acid polymers, Biochim. Biophys. Acta (BBA)-Biomembr. 1860 (2) (2017) 257–263.
[19] M. Jamshad, et al., G-protein coupled receptor solubilization and purification for biophysical analysis and functional studies, in the total absence of detergent, Biosci. Rep. 35 (2) (2015) e00188.
[20] S. Gulati, et al., Detergent-free purification of ABC (ATP-binding-cassette) transporters, Biochem. J 461 (2) (2014) 269–278.
[21] D.J. Swainsbury, et al., Bacterial reaction centers purified with styrene maleic acid copolymer retain native membrane functional properties and display enhanced stability, Angew. Chem. Int. Ed. Engl. 53 (44) (2014) 11803–11807.
[22] J.M. Dörr, et al., Detergent-free isolation, characterization, and functional reconstitution of a tetrameric K+ channel: the power of native nanodiscs, Proc. Natl. Acad. Sci. 111 (52) (2014) 18607–18612.
[23] C. Logez, et al., Detergent-free isolation of functional G protein-coupled receptors into nanometric lipid particles, Biochemistry 55 (1) (2015) 38–48.
[24] K.A. Morrison, et al., Membrane protein extraction and purification using styrene-maleic acid (SMA) copolymer: effect of variations in polymer structure, Biochem. J. 473 (23) (2016) 4349–4360.
[25] M. Jamshad, et al., Surfactant-free Purification of Membrane Proteins with Intact Native Membrane Environment, Portland Press Limited, 2011.
[26] C. Vargas, et al., Nanoparticle self-assembly in mixtures of phospholipids with styrene/maleic acid copolymers or fluorinated surfactants, Nanoscale 7 (48) (2015) 20685–20696.
[27] S. Scheidelaar, et al., Molecular model for the solubilization of membranes into nanodisks by styrene maleic acid copolymers, Biophys. J. 108 (2) (2015) 279–290.
[28] R.C. Arenas, et al., Influence of lipid bilayer properties on nanodisc formation mediated by styrene/maleic acid copolymers, Nanoscale 8 (32) (2016) 15016–15026.
[29] T. Ravula, et al., pH tunable and divalent metal ion tolerant polymer lipid nanodiscs, Langmuir 33 (40) (2017) 10655–10662.
[30] D.A. Jacques, J. Trewhella, Small-angle scattering for structural biology—Expanding the frontier while avoiding the pitfalls, Protein Sci. 19 (4) (2010) 642–657.
[31] P.V. Konarev, et al., PRIMUS: a Windows PC-based system for small-angle scattering data analysis, J. Appl. Crystallogr. 36 (5) (2003) 1277–1282.
[32] D. Svergun, Determination of the regularization parameter in indirect-transform methods using perceptual criteria, J. Appl. Crystallogr. 25 (4) (1992) 495–503.
[33] A.G. Kikhney, D.I. Svergun, A practical guide to small angle X-ray scattering (SAXS) of flexible and intrinsically disordered proteins, FEBS Lett. 589 (19PartA) (2015) 2570–2577.
[34] A. Guinier, The diffusion of x-rays under the extremely weak angles applied to the study of fine particles and colloidal suspension, C. R. Hebdomadaires Des Seances De L Academie Des Sci. 206 (1938) 1374–1376.
[35] A. Guinier, G. Fournet, C. Walker, Small Angle Scattering of X-rays, J. Wiley & Sons, New York, 1955.
[36] O. Glatter, Data evaluation in small angle scattering: calculation of the radial electron density distribution by means of indirect Fourier transformation, Acta Phys. Austriaca 47 (1–2) (1977) 83–102.
[37] J. Perez, et al., Heat-induced unfolding of neocarzinostatin, a small all-β protein investigated by small-angle X-ray scattering1, J. Mol. Biol. 308 (4) (2001) 721–743.
[38] V. Graziano, L. Miller, L. Yang, Interpretation of solution scattering data from lipid nanodiscs, J. Appl. Crystallogr. 51 (Pt 1) (2018) 157–166.
[39] E. Walenta, Small angle x-ray scattering. Von O. GLATTER und O. KRATKY. London: Academic Press Inc. Ltd. 1982. ISBN 0-12-286280-5. X, 515 Seiten, geb. £ 43,60; US $ 81.00, Acta Polym. 36 (5) (1985) 296–296.
[40] T. Zheltonozhskaya, et al., Influence of the reaction temperature on the structure of the polycomplexes of the copolymer of styrene and maleic acid with polyoxyethylene, Polym. Sci. USSR 29 (12) (1987) 2735–2743.
[41] P. Demchenko, V. Boiko, Investigation of conformational changes in styrene-maleic acid copolymer macromolecules during ionization in aqueous solutions, Polym. Sci. USSR 15 (10) (1973) 2626–2634.
[42] S. Ulrich, A. Laguecir, S. Stoll, Titration of hydrophobic polyelectrolytes using Monte Carlo simulations, J. Chem. Phys. 122 (9) (2005) 094911.
[43] S. Scheidelaar, et al., Effect of polymer composition and pH on membrane solubilization by styrene-maleic acid copolymers, Biophys. J. 111 (9) (2016) 1974–1986.
[44] M. Das, et al., Rationally engineered tandem facial amphiphiles for improved membrane protein stabilization efficacy, ChemBioChem 19 (20) (2018) 2225–2232.

Further reading

[45]
Nathan Brady, N.G. Brady et al. SAXS Data of SMA Copolymers in Solution, Mendeley Data, v2, 2018 < https://doi.org/10.17632/zv7mzsrd5r.2 > .